Journal of Luminescence 202 (2018) 20–26

Contents lists available at ScienceDirect

Journal of Luminescence

journal homepage: www.elsevier.com/locate/jlumin

Carrier dynamics in hybrid nanostructure with electronic coupling from an InGaAs quantum well to InAs quantum dots

Ying Wang[a,b,*], Xinzhi Sheng[a], Qing Yuan[b], Qinglin Guo[b], Shufang Wang[b], Guangsheng Fu[b], Baolai Liang[c,*], Diana L. Huffaker[c], Yuriy I. Mazur[d], Yurii Maidaniuk[d], Morgan E. Ware[d], Gregory J. Salamo[d]

[a] *School of Science, Beijing Jiaotong University, Beijing 100044, PR China*
[b] *College of Physics Science & Technology, Hebei University, Baoding 071002, PR China*
[c] *California NanoSystem Institute, University of California - Los Angeles, CA 90095, USA*
[d] *Institute for Nanoscience and Engineering, University of Arkansas, AR 72701, USA*

ARTICLE INFO

Keywords:
Carrier dynamics
Resonant carrier tunneling
Photoluminescence
Quantum dots
Quantum well

ABSTRACT

Carrier dynamics including carrier relaxation and tunneling within a coupled InAs quantum dot (QD) – $In_{0.15}Ga_{0.85}As$ quantum well (QW) hybrid nanostructure are investigated using photoluminescence (PL) spectroscopy. This coupled hybrid nanostructure shows a single PL peak from the QD emission at low excitation intensity and a band filling behavior is observed as the excitation intensity increases, suggesting that there exists a channel to capture carriers from the QW to the QDs. Time resolved PL (TRPL) measurements extract a carrier tunneling time of 103.7 ps, which is only one third of the theoretical prediction. A double-channel resonant carrier tunneling mechanism from the QW to the wetting layer and to the fifth excited state of the QDs and then carrier relaxation into lower discrete QD energy states is proposed to explain this fast carrier tunneling. The double-channel resonant carrier tunneling mechanism is qualitatively supported through the analysis of the excitation-dependent PL spectra as well as the PL excitation spectra. These results enrich our understanding of carrier dynamics in coupled QD and QW hybrid structures.

1. Introduction

Since 1993, self-assembled quantum dots (QDs) grown by the Stranski-Krastanow (S-K) strain relaxation have gained great attention due to their possible optoelectronic device applications, such as semiconductor lasers, amplifiers, modulators, photovoltaic, and infrared photo-detectors [1–6]. As examples, QD hybrid structures with QDs coupled to a quantum well (QW) have been exploited in various material systems and optoelectronic devices where additional excess carriers can be provided through carrier transfer from the QW [7–14]. There are at least two ways to fabricate such QD hybrid systems. The first, a so-called dot in well (DWELL) structure, immerses QDs directly into a QW. This has been well studied and used to modify the performances for QD lasers, photodetectors, and intermediate-band solar cells [15–18]. A second approach is to architect the “injection-structure” by separating the QD layer from the QW with a thin barrier. This approach is particularly interesting because it allows for more independent control of the QDs, as well as the ability to inject carriers from the QW to the QDs [19–22]. The nanostructures obtained via this second approach have been explored most recently to improve the device performance for lasers and photovoltaics [22,23]. In view of the significance of the applications and the complexities of the structures, carrier dynamics play a very important role in the improvement of device performances while carrier injection and processes involved in vertical and lateral transfer have been well investigated for several hybrid systems. In this paper, we report comparison studies on two hybrid structures with InAs QDs coupled and uncoupled to an InGaAs QW. The emission characteristics for these two samples are investigated by excitation intensity and temperature dependent PL together with time-resolved PL (TRPL). A fast carrier tunneling is experimentally observed and a double-channel resonant carrier tunneling mechanism from the QW to the wetting layer and to the discrete energy states of the QDs is proposed to explain the observed fast carrier tunneling.

2. Sample structures and MBE growth

The hybrid structures were grown by a solid source molecular beam epitaxy (MBE). As shown in Fig. 1(a), for the coupled sample A, a

---

* Corresponding authors.
E-mail addresses: hbuwangying@hbu.edu.cn (Y. Wang), bliang@cnsi.ucla.edu (B. Liang).

https://doi.org/10.1016/j.jlumin.2018.05.029
Received 12 December 2017; Received in revised form 2 May 2018; Accepted 10 May 2018

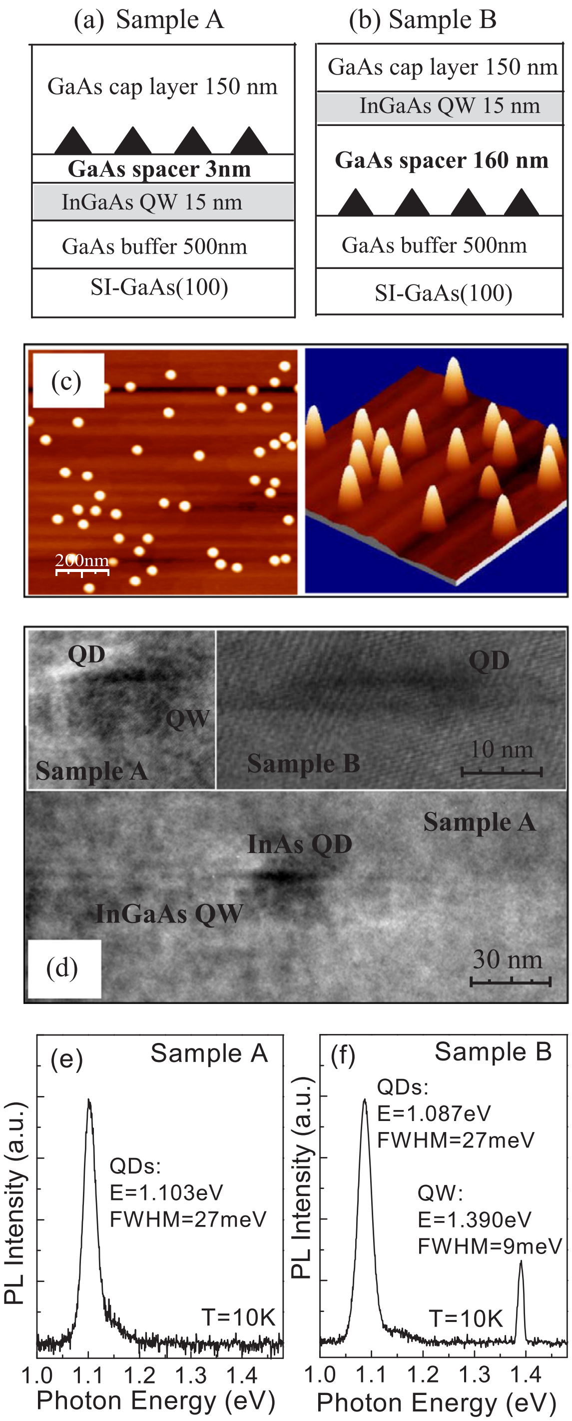

Fig. 1. (a) and (b) are the schematic diagrams of the hybrid structures for coupled sample A and uncoupled sample B, respectively; (c) 1 µm × 1 µm AFM image of the InAs QDs with an enlarged 0.5 µm × 0.5 µm 3D view; (d) TEM images of InAs QDs in both samples A and B; (e) and (f) show the PL spectra of the two samples measured at T = 10 K with an excitation intensity of P = 10 mW/cm^2.

500 nm GaAs buffer layer was grown on a semi-insulating GaAs (001) substrate at 580 °C, then a 15 nm In$_{0.15}$Ga$_{0.85}$As QW layer grown at a substrate temperature of 520 °C, followed by a 3 nm GaAs spacer at 520 °C and 1.8 monolayers (ML) of InAs at 520 °C which form QDs through S-K relaxation, and finally a 150 nm GaAs capping layer was grown at 580 °C. An uncoupled sample B was grown using the same growth conditions except that the QD and QW layers are inverted in the layer order with a 160 nm spacer between them, as shown in Fig. 1(b). This inversion was chosen in order that the QW PL is not absorbed by the lower energy QDs. With the assumptions that the QD layer is pseudomorphic, i.e., introduces no new defects, and that the 160 nm spacer is sufficiently large such that strain from the QDs do not influence the growth of the QW, we believe that this inversion will have no other effects on the results.

As reference, a sample with QDs formed from the deposition of 1.8 ML of InAs at 520 °C and no capping is grown for morphology study by Atomic Force Microscope (AFM). As shown in Fig. 1(c), the uncapped QDs were measured to have an areal density of $\sim 4.8 \times 10^9$ cm^{-2}, an average height of 11.5 nm, and an average diameter of 46.8 nm. Defects or large incoherent islands are not found on the surface of the sample, indicating high quality, pseudomorphic QDs. It is well known that the dimensions and shape of the InAs QDs will change significantly after the QDs are capped. As shown in Fig. 1(d), the cross-sectional Transmission Electron Microscopy (TEM) images show much smaller InAs QDs with a diameter of ~ 20 nm and a height of ~ 2.5 nm for both sample A and sample B in comparison with the QDs observed by AFM. The QD dimensions measured by TEM rather than by AFM were subsequently used to obtain reasonable band structure calculations using the semiconductor simulation package, Nextnano. The coupled structure between QDs and QW via a 3 nm GaAs spacer is also confirmed for sample A by the TEM images.

3. Results and disscussion

For PL measurements, samples were excited by a continuous-wave 532 nm laser, i.e., with energy is well above the GaAs band gap. Therefore, the photon-excited carriers are mainly generated in the GaAs matrix, then relax into the QW and the QDs. The PL spectra for both samples were first measured at low temperature (T = 10 K) with the low excitation intensity of 10 mW/cm^2 to avoid saturation effect. As shown in Fig. 1(e), sample A has a single peak from QD emission at 1.103 eV with a Full-Width-at-Half-Maximum (FWHM) of 27 meV. In comparison, sample B has shown a QD peak at 1.087 eV with a FWHM of 27 meV and a narrow QW peak at 1.390 eV with a FWHM of 9 meV. Here we find that the PL from the QDs in both samples have very similar emission energy and linewidth. However, we will show that the QW peak from Sample A is absent due to rapid carrier transfer to the QDs.

Subsequently, examining the PL as a function of laser excitation intensity shows how the available states fill and emit. This is shown in Fig. 2(a) and (b) for samples A and B, respectively. We see here, that the overall structure of the excitation intensity dependencies from these two samples are generally quite similar in that they both show a classical state filling progression of the QD peaks. However, we find that the states fill remarkably faster with increasing power in sample A where the QDs and QW are coupled than they do in sample B where they are uncoupled. Additionally, the initially absent QW peak from sample A appears at ~ 1.39 eV and increases in intensity rapidly. Finally, at the highest excitation intensities, we see a high energy shoulder become prominent at ~ 1.43 eV in both samples. This is most likely the emission from the QD wetting layer or the excited states of the QW. Due to the quick increase in intensity of the QW peak in sample A, we conclude that there is an efficient channel for carrier relaxation from the GaAs matrix to the QW and then to the QDs [24]. Therefore, it is only after the QDs are sufficiently filled that the QW emission peak turns on. Here, the QW plays the role of a reservoir to efficiently collect photon-generated carriers from the GaAs matrix and pass them to the QDs, although the carrier generation and carrier relaxation in the QW as well as in the QDs also exist. Following this, the carriers begin to quickly populate the QW energy states after the lower energy levels of the QDs have been filled, according to the calculated band diagram shown in Fig. 2(c).

The integrated PL intensity of the QW and of the QDs for sample B, as well as their ratio (QW/QDs) are extracted and plotted in Fig. 2(d) as